Chapter Three
Mathematical model

3.1 Introduction

In this chapter all the mathematical model for each hybrid system wind system, PV solar system and diesel backup generator is presented.

3.2 Wind turbine model

The speed of rotation of a wind turbine is usually measured in either rotation speed in revolutions per minute (N in rpm) or angular velocity in radians per second (ω in rad/s) **.**The relationship between the two is given by**:**

$$\omega = 2 * \pi * N/60 \qquad (3.1)$$

Another measure of a wind turbine's speed is its tip speed, ν, which is the tangential velocity of the rotor at the tip of the blades measured in meter per second and it equals to:

$$\nu = \omega * r \qquad (3.2)$$

where r is the tip radius in meters.

A non-dimensional ratio known as the tip speed ratio (TSR) is obtained by dividing the tip speed, ν, by the undisturbed wind speed, V_o. This ratio which provides a useful measure can be used to compare wind turbines of different characteristics.

$$TSR = \omega * r/V_o \qquad (3.3)$$

A wind turbine of a particular design can operate over a range of tip speed ratios, but will usually operate with its best efficiency at a particular tip speed ratio. The optimum tip speed ratio for a given wind turbine rotor will depend upon both the number of blades and the width of each blade.

Consider a (packet) of air with mass *m* moving at a speed *v*. Its kinetic energy

K.E. is given by the familiar relationship:

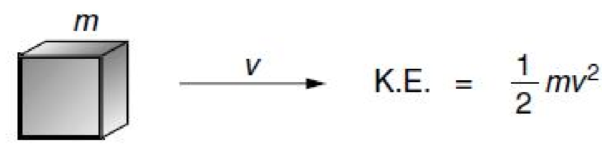

Since power is energy per unit time, the power represented by a mass of airmoving at velocity *v* through area *A* will be

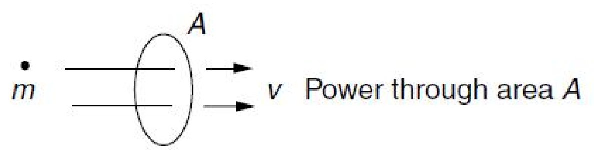

$$Power\ through\ area\ A = \frac{\text{Energy}}{Time} = \frac{1}{2}\left(\frac{Mass}{Time}\right)v^2 \qquad (3.4)$$

The mass flow rate $\dot{m}$, through area *A*, is the product of air density ρ, speed *v*, and cross-sectional area *A*:

$$\frac{(mass\ passing\ through\ A)}{time} = \dot{m} = \rho A v \qquad (3.5)$$

Notice that the power in the wind increases as the *cube* of wind speed. This means, for example, that doubling the wind speed increases the power by eight fold. Equation (3.4) also indicates that wind power is proportional to the swept area of the turbine rotor [4].

For a conventional horizontal axis turbine, the area A is obviously just *A* = $(D^2\pi/4)$, so wind power is proportional to the square of the blade diameter. Doubling the diameter increases the power available by a factor of four [4].

The swept area of a vertical axis Darrieus rotor is a bit more complicated to figure out. One approximation to the area is that it is about two-thirds the area of a rectangle with width equal to the maximum rotor width and height equal to the vertical extent of the blades, as shown in Figure 3.1 [4].

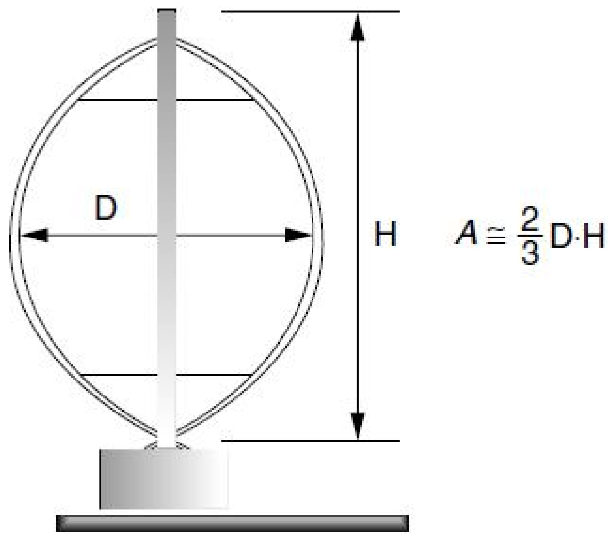

Figure 3.1: Showing the approximate area of a Darrieus rotor.

That simple observation helps explain the economies of scale that go with larger wind turbines. The cost of a turbine increases roughly in proportion to blade diameter, but power is proportional to diameter squared, so bigger machines have proven to be more cost effective.

Several studies have been reported regarding to WT and wind generators. In this study, the proposed WT model is based on the wind speed versus WT output power characteristics. Combining (3.4) with (3.5) gives us an important relationship

$$P_m = c_p(\lambda, \beta) \frac{\rho A}{2} {v^3}_{wind} \qquad (3.6)$$

Where:

Pm: is the mechanical output power of the turbine,

Cp: is the performance coefficient of the turbine,

λ :is the tip speed ratio of the rotor blade,

β: is the blade pitch angle,

ρ: is the air density,

A: is the turbine swept area,

υ_{wind}: is the wind speed.

The performance coefficient model Cp (λ,β) used in this paper is taken from [7] and given by:

$$c_p(\lambda,\beta) = c_1\left(\frac{c_2}{\lambda_i} + c_3\beta - c_4\right)e^{-c5/\lambda i} + c_6\,\lambda \qquad (3.7)$$

Where

Constants c_1 to c_6 are parameters that depend on the wind turbine rotor and blade design,

λi :is a parameter given in [7].

$$\frac{1}{\lambda_i} = \frac{1}{\lambda + 0.08\,\beta} - \frac{0.035}{\beta^3 + 1} \qquad (3.8)$$

The based wind speed is the mean value of the expected wind speed in (m/s).

The modified model of the WT is implemented as shown in Figure 3.2. In this model, whereas the inputs are the wind speed and generator speed, the output is the torque applied to the generator shaft. The torque of the generator is based on the generator power and speed.

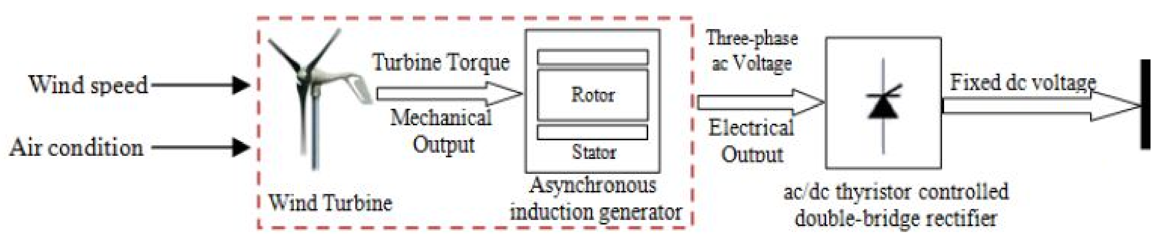

Figure 3.2: Block diagram of the proposed wind system

3.2.1 Wind Turbine Induction Generator:

The Induction Generator is provided with two windings, one on the stator, and one on the rotor. The stator winding of the induction motor has two functions. It provides the excitation or magnetization, and carries the armature or generated current. The rotor winding carries the armature current only. When AC excitationis present, the magnetic field created rotates at a speed determined jointly by the number of poles in the winding and the frequency of the current, the synchronous speed [8].

If the rotor rotates at a speed other than the synchronous speed, voltage is generated in the rotor winding at a frequency corresponding to the difference in the two frequencies, known as the slip frequency. This voltage drives the armature current, and provided the rotor speed is faster than the synchronous speed, the machine acts as a generator. The function is thus asynchronous [8].

The steady state equivalent circuit of IG is shown in Figure 3.3 [8]:

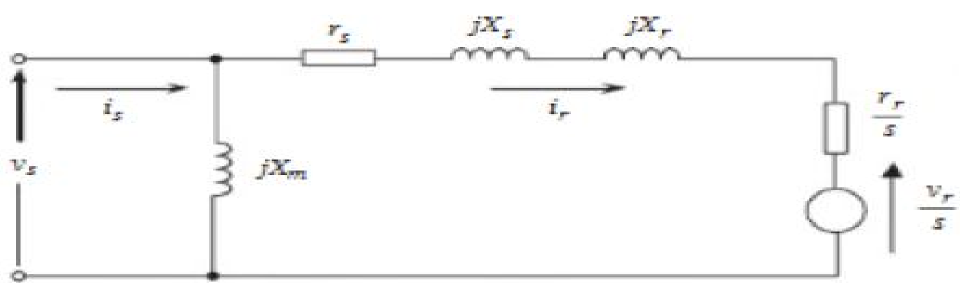

Figure 3.3: steady state equivalent circuit of IG

To obtain the torque equation from the equivalent circuit, we can simplify the steady state induction motor circuit by moving Xm to the stator terminal. The rotor current I_r is expressed as [8]:

$$\mathrm{I_r} = \frac{V_s - \left(\frac{V_r}{s}\right)}{\left(r_s + \frac{r_r}{s}\right) + \mathrm{j}(X_s + \mathrm{X_r})} \tag{3.9}$$

The electrical torque Te, from the power balance across the stator to rotor gap, can be calculated from:

$$\mathrm{Te} = \mathrm{Ir}^2 \frac{\mathrm{r_r}}{\mathrm{s}} + \frac{\mathrm{P_r}}{\mathrm{s}} \tag{3.10}$$

Where the power supplied or absorbed by the controllable source injecting voltage into the rotor circuit, that is the rotor active power, Pr can be calculated from:

$$P_r = \frac{V_r}{s} I_r \cos\theta \tag{3.11}$$

3.2.2 Wind Turbine Control System

Due to the variations in wind speed, the output power of the wind turbine induction generator experiences variations in frequency and amplitude. Therefore, a controllable ac/dc converter is used to smooth the wind turbine output power before being supplied to other electronic devices [7].

One of the advantages of the double-bridge rectifier is the controllable dc output voltage, by tuning the firing angle (α) of the 12-pulse synchronized PWM generator, and the narrowed commutation periods, which causes less harmonic distortion effects on the source side. In this model a three-phase two winding transformer is used to obtain six input ports with appropriate phase angles for the double-bridge rectifier. The firing angle (α) is controlled by a discrete PI controller, firing angle of the bridge rectifier is given by [7]:

$$\cos(\alpha) = \frac{V_{d\alpha}\,\pi}{3 * \sqrt{3} * V_m} \tag{3.12}$$

Where:

$V_{d\alpha}$: is the output voltage of the rectifier

V_m: is the maximum voltage

α: firing angle

For the inductance filter, if the V_{dc} is less than V_m, the current i_0 begins to flow at α which is given by [9]:

$$V_{dc} = V_m \sin \alpha \tag{3.13}$$

This in turn gives:

$$\alpha = \sin^{-1}\frac{V_{dc}}{V_m} = \sin^{-1} x \tag{3.14}$$

Where $x = \frac{Vdc}{Vm}$. The output current i_0 is given by

$$Le\,\frac{dil}{dt} = V_m \sin \omega t - V_{dc}$$

Which can be solved for i_0.

$$i_0 = \frac{1}{\omega L_e}\int_{\alpha}^{\omega t} (V_m \sin \omega t - V_{dc})\, d(\omega t) \tag{3.15}$$

The average current can be found from:

$$i_{dc} = \frac{1}{\pi}\int_{\alpha}^{\pi+\alpha} i_0(t)\, d(\omega t) \tag{3.16}$$

After integration and simplified gives:

$$i_{dc} = \frac{V_m}{\omega L_e}\left[\sqrt{1-x^2} + \frac{2}{\pi} - \frac{\pi}{2}\right] \tag{3.17}$$

Because the average voltage of rectifier is $V_{dc}=2V_m/\pi$, the average current equal

$$i_{dc} = \frac{2V_m}{\pi R} \tag{3.18}$$

Thus:

$$\frac{2V_m}{\pi R} = i_{dc} = \frac{V_m}{\omega L_e}\left[\sqrt{1-x^2} + \frac{2}{\pi} - \frac{\pi}{2}\right] \tag{3.19}$$

Which gives the critical value of the inductance $L_{cr} = L_e$ for continuous current

$$L_e > L_{cr} = \frac{\pi R}{2\omega}\left[\sqrt{1-x^2} + \frac{2}{\pi} - \frac{\pi}{2}\right] \tag{3.20}$$

The equations of discrete PI controller are:

$$G(s) = K_P + \frac{K_I}{S} \tag{3.21}$$

The proposed wind turbine control system model is implemented as shown in Figure 3.4.

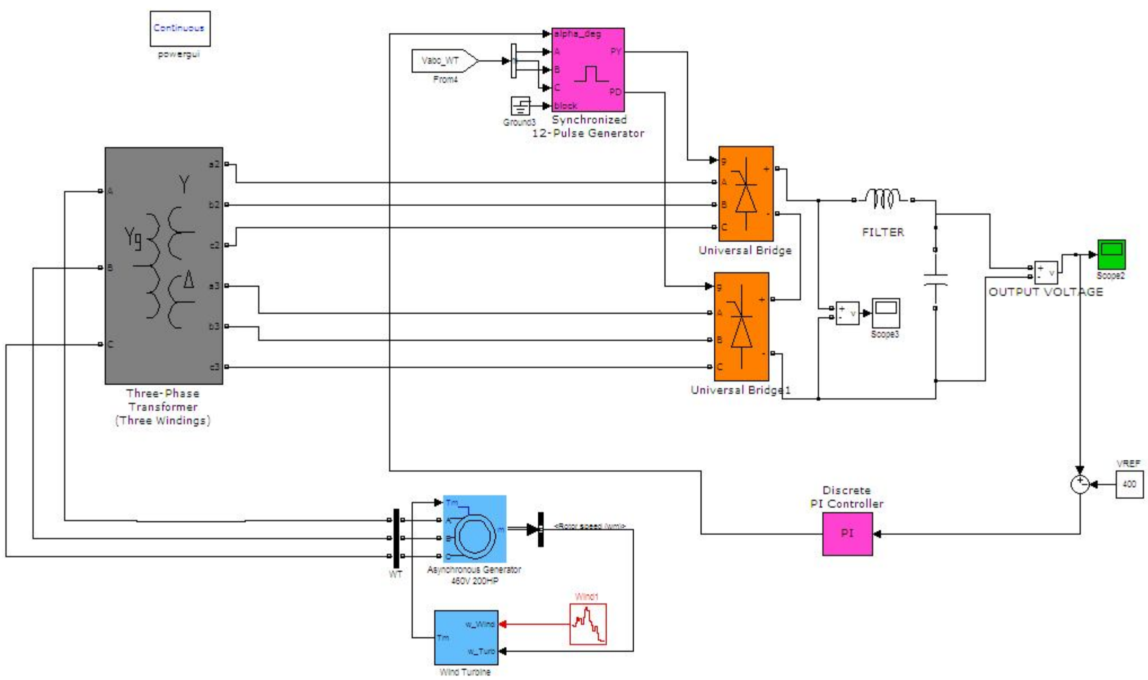

Figure 3.4: Wind Turbine system model

3.3 Modeling of diesel generator

Ac generators or alternators operate in the same fundamental principles of electromagnetic induction as dc generators. They also consist of an armature winding and magnetic field, but there is one important difference between the two. Whereas in dc generators, the armature rotates and field system is stationary, the arrangement in alternators is just the reverse of it. In their case, standard construction consists of armature winding mounted on stationary element called stator and field winding on rotating element called rotor. The Figure 3.5 shows the scheme of synchronous machine [10].

The type of rotor used for this model is smooth cylindrical or round, it is used for steam turbine –driven alternators that is turbo –alternator, which run at very high speeds. The rotor consists of a smooth solid force steel cylinder, having number of slots milled out at intervals along the outer periphery (and parallel to the shaft) for accommodating field coils. Such rotors are designed mostly for 2 pole or 4 poles turbo generators running at 4600 rpm. (Or 1800 rpm) two or four regions corresponding to the central polar areas are left unslotted [10].

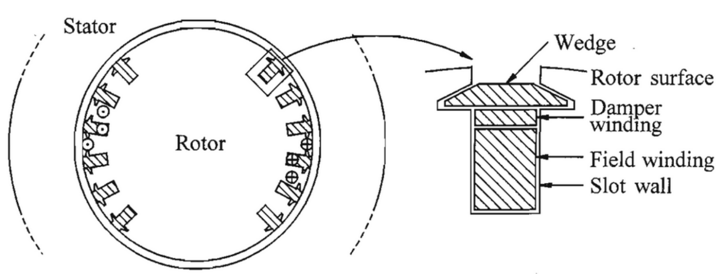

Figure 3.5: Three phase synchronous machine round rotor

Nearly all of the electric power used throughout the world is generated by synchronous machines driven either by hydro or steam turbines or by combustion engines. Just as the induction machine is the workhorse when it comes to converting energy from electrical to mechanical, the synchronous machine is the principal means of converting energy from mechanical to electrical.

The electrical and electromechanical behavior of most synchronous machines can be predicted from the equations that describe the 3-phase salient-pole synchronous machine. In particular, these equations can be used directly to predict the performance of hydro and steam turbine synchronous generators, synchronous motors, and-with only slight modifications reluctance motors [10].

From the mathematical model shown below the impedance of the three phase synchronous generator can be obtained as flow:

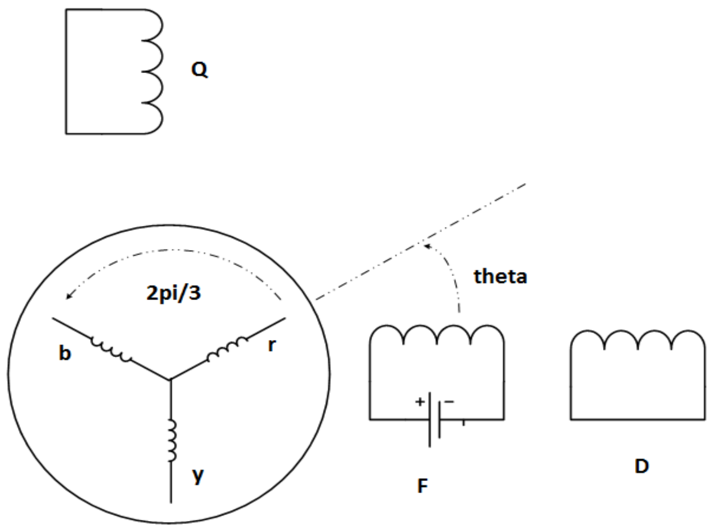

$$[Z] = \begin{bmatrix} R_F + L_F P & M_{FD} P & 0 & \hat{M}_F P\cos\theta & \hat{M}_F P\cos\theta 2 & \hat{M}_F P\cos\theta 3 \\ M_{DF} P & R_D + L_D P & 0 & \hat{M}_D P\cos\theta & \hat{M}_D P\cos\theta 2 & \hat{M}_D P\cos\theta 3 \\ 0 & 0 & R_Q + L_Q P & \hat{M}_Q P\sin\theta & \hat{M}_Q P\sin\theta 2 & \hat{M}_Q P\sin\theta 3 \\ \hat{M}_F P\cos\theta & \hat{M}_D P\cos\theta & \hat{M}_Q P\sin\theta & R_r + PL_r & PMry & PMrb \\ \hat{M}_F P\cos\theta 2 & \hat{M}_D P\cos\theta 2 & \hat{M}_Q P\sin\theta 2 & PMry & R_y + PL_y & PMyb \\ \hat{M}_F P\cos\theta 3 & \hat{M}_D P\cos\theta 3 & \hat{M}_Q P\sin\theta 3 & PMbr & PMby & R_b + PL_b \end{bmatrix} \tag{3.22}$$

$$V = ZI \tag{3.23}$$

Therefore:

$$\begin{bmatrix} VF \\ VD \\ VQ \\ Vr \\ Vy \\ Vb \end{bmatrix} = \begin{bmatrix} R_F + L_F P & M_{FD} P & 0 & \hat{M}_F P\cos\theta & \hat{M}_F P\cos\theta 2 & \hat{M}_F P\cos\theta 3 \\ M_{DF} P & R_D + L_D P & 0 & \hat{M}_D P\cos\theta & \hat{M}_D P\cos\theta 2 & \hat{M}_D P\cos\theta 3 \\ 0 & 0 & R_Q + L_Q P & \hat{M}_Q P\sin\theta & \hat{M}_Q P\sin\theta 2 & \hat{M}_Q P\sin\theta 3 \\ \hat{M}_F P\cos\theta & \hat{M}_D P\cos\theta & \hat{M}_Q P\sin\theta & R_r + PL_r & PMry & PMrb \\ \hat{M}_F P\cos\theta 2 & \hat{M}_D P\cos\theta 2 & \hat{M}_Q P\sin\theta 2 & PMry & R_y + PL_y & PMyb \\ \hat{M}_F P\cos\theta 3 & \hat{M}_D P\cos\theta 3 & \hat{M}_Q P\sin\theta 3 & PMbr & PMby & R_b + PL_b \end{bmatrix} \begin{bmatrix} IF \\ ID \\ IQ \\ Ir \\ Iy \\ Ib \end{bmatrix} \tag{3.24}$$

3.4 Modeling of a Photovoltaic Module

The general mathematical model for the solar cell has been studied over the past three decades. The circuit of the solar cell model, which consists of a photocurrent, diode, parallel resistor (leakage current) and a series resistor; is shown in Figure 3.6. According to the PV cell circuit shown in Figure 3.7 and Kirchhoff's current laws, the photovoltaic current can be presented as follows [7]:

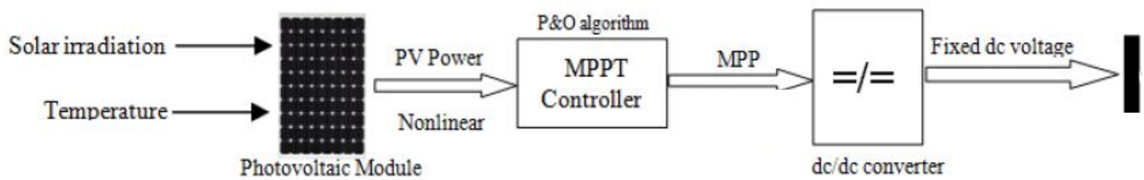

Figure 3.6: Block diagram of the proposed solar system

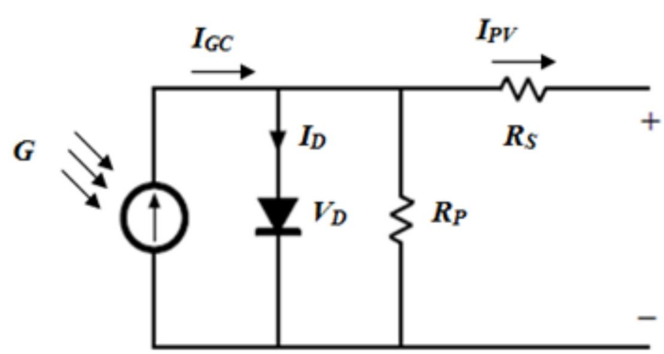

Figure 3.7: The Simplest Equivalent Circuit for a Photovoltaic Cell

$$I_{pv} = I_{gc} - I_0\left[exp^{[\frac{ev_d}{KFTc}]} - 1\right] - \frac{v_d}{R_p} \qquad (3.25)$$

Where:

Igc: is the light generated current,

Io: is the dark saturation current dependent on the cell temperature,

E: is the electric charge = 1.6 x 10-19 Coulombs,

K: is Boltzmann's constant = 1.38 x 10-23 J/K, F: is the cell idealizing factor,

Tc: is the cell's absolute temperature,

Vd: is the diode voltage, and Rp is the parallel resistance.

The photocurrent (Igc) mainly depends on the solar irradiation and cell temperature, which is described as:

$$I_{gc} = [\mu sc\ (Tc - Tr) + \ Isc]G \tag{3.26}$$

Where:

μsc :is the temperature coefficient of the cell's short circuit current,

Tref: is the cell's reference temperature,

Isc :is the cell's short circuit current at a 25^0C and 1kW/m2,

G : is the solar irradiation in kW/m2.

Furthermore, the cell's saturation current (Io) varies with the cell temperature, which is described as

$$I_o = I_{o\alpha}\left(\frac{Tc}{Tr}\right)^3 exp^{\left[\frac{ev_g}{KF}\left(\frac{1}{Tr}-\frac{1}{Tc}\right)\right]} \tag{3.27}$$

$$I_{o\alpha} = \frac{Isc}{exp^{\left[\frac{ev_{OC}}{KFTc}\right]} - 1} \tag{3.28}$$

Where:

Ioα: is the cell's reverse saturation current at a solar radiation and reference temperature

Vg :is the band-gap energy of the semiconductor used in the cell,

Voc: is the cells open circuit voltage

The block diagram to simulate this model is shown in Figure 3.8:

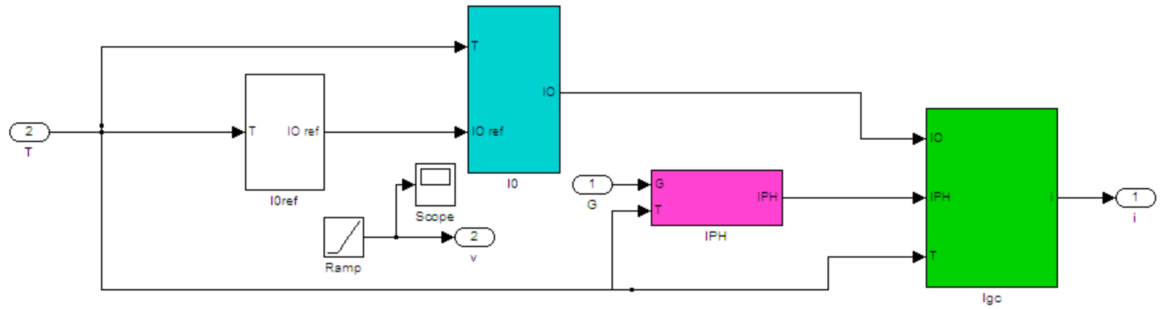

Figure 3.8: PV system model

3.4.1 PV Maximum power point tracker (MPPT)

Specific commands laws existing to bring devices to operate at maximum points of their characteristics without neither the knowledge in advance of these points nor the knowledge when they have been changed or what are the reasons for this change. This type of control is often referred to as maximum power point tracking (MPPT). The principle of these commands is to conduct a search of the point of maximum power while ensuring a perfect matching between the generator and load [11].

From the power processing point of view, high efficiency conversion, by itself, cannot ensure the optimized power flow, since the PV output voltage and current are strongly dependent on environmental conditions, that is solar radiation and temperature; however, on the literature, many works bring solutions to maximize the photovoltaic output power, employing specific circuits denominated by Maximum Power Point Trackers (MPPT). In most applications, the MPPT is a simple dc-dc converter interposed between the photovoltaic modules and the load, and its control is achieved through a tracking algorithm [12].

A lot of MPPT algorithms have been developed by researchers and industry delegates all over the world. They are voltage feedback method, perturbation and observation method, linear approximation method, incremental conductance method, hill climbing method, actual measurement method, fuzzy control method and so on [13].

In MPPT, most control scheme use the P&O technique because it is easy to implement [14] which is used in this project.

3.4.2 Perturbation and Observation Method (P&O):

P&O method is the most frequently used algorithm to track the maximum power due to its simple structure and fewer required parameters. This method finds the maximum power point of PV modules by means of iteratively perturbing, observing and comparing the power generated by the PV modules. It is widely applied to the maximum power point tracker of the photovoltaic system for its features of simplicity and convenience [13].

According to the structure of MPPT system shown in Figure 3.9, the required parameters of the power-feedback type MPPT algorithms are only the voltage and current of PV modules. Figure 3.10 is the relationship between the terminal voltage and output power generated by a PV module. It can be observed that regardless of the magnitude of sun irradiance and terminal voltage of PV modules, the maximum power point is obtained while the condition $dP/dV = 0$ is accomplished. The slope (dP/dV) of the power can be calculated by the consecutive output voltages and currents [13].

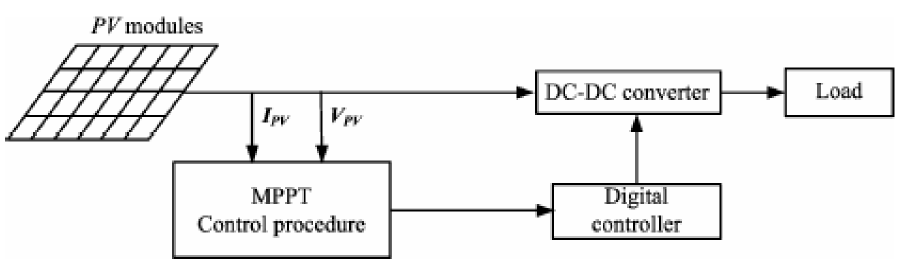

Figure 3.9: A structure of PV system with MPPT function

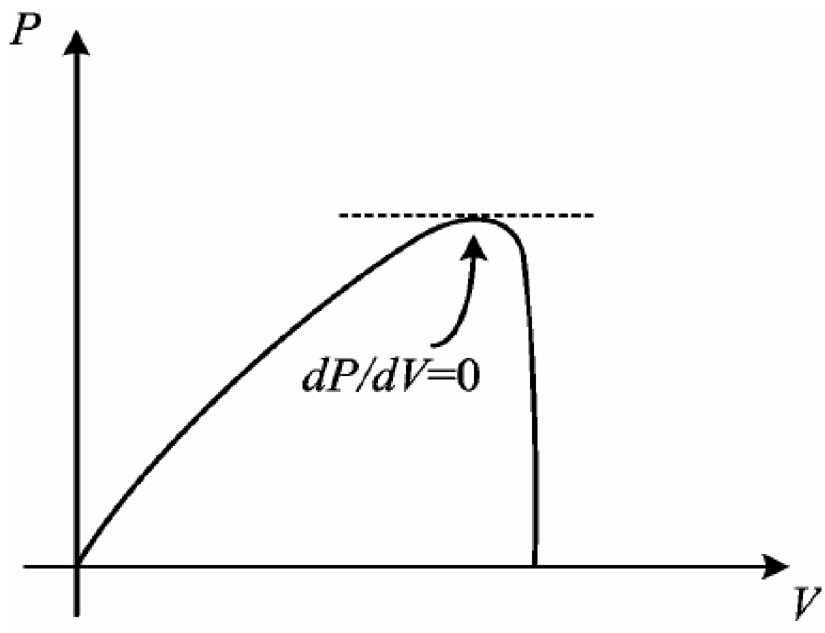

Figure 3.10: PV characteristic of a PV model

In a fixed period of time, the load of the PV system is adjusted in order to change the terminal voltage and output power of the PV modules. The variations of the output voltage and power before and after changes are then observed and compared to be the reference for increasing or decreasing the load in the next step. If the perturbation in this time results in greater output power of PV modules than that before the variation, the output voltage of PV modules will be varied toward the same direction.

Otherwise, if the output power of PV modules is less than that before variation, it indicates that the varying direction in the next step should be changed. The maximum output power point of a PV system can be obtained using these iterative perturbation, observation and comparison steps [13].

The advantages of the P&O method are simple structure, easy implementation and less required parameters. The shortcomings of the P&O method can be summarized as the power tracked by the P&O

method will oscillate and perturb up and down near the maximum power point. The basic operating procedure of P&O method is shown in Figure 3.11[13].

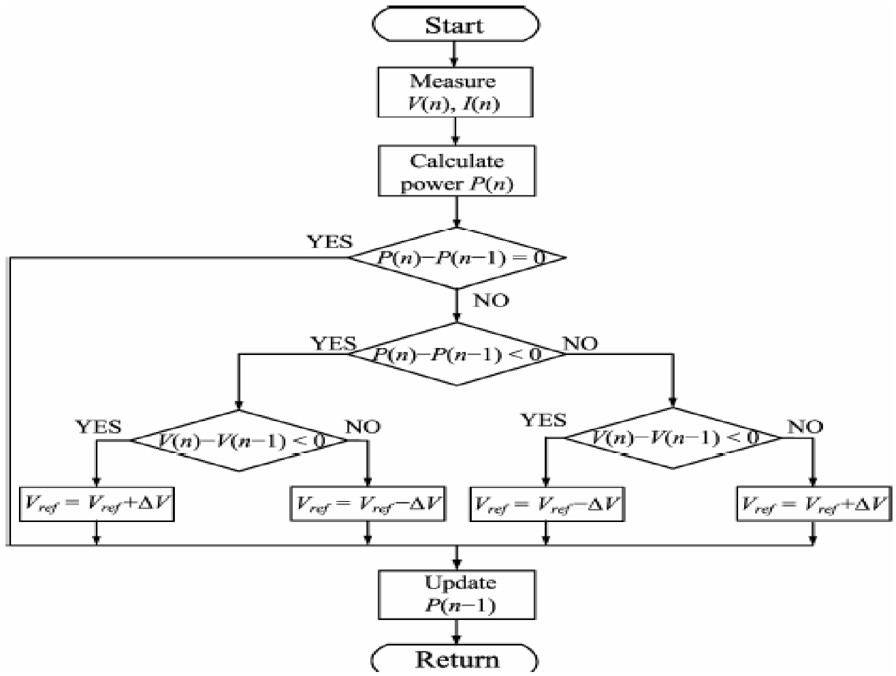

Figure 3.11: The flow diagram of the P&O method

3.4.3 Dc /Dc converter

In addition, a dc averaged switched model converter with input current control (Iref and Vref) is built and implemented using MATLAB/SIMULINK, to reduce the switching harmonics and steps-up the photovoltaic voltage to a higher dc voltage (e.g. 400V) using the boost regulators .

According to equations of boost converter [9]:

$$\frac{Vs}{Va} = (1 - D) \tag{3.29}$$

Where :

Vs: the input voltage of the boost regulator

Va: the output voltage of the boost regulator

D: duty cycle

$$Is = \frac{Ia}{(1-D)} \tag{3.30}$$

Is: the input current of the boost regulator

Ia: the output current of the boost regulator

Assuming lossless circuit:

$$VsIs = Va\,Ia = Vs\frac{Ia}{(1-D)} \tag{3.31}$$

When the transistor is on, the capacitor supplies the load current. The average capacitor current during time t1 is Ic = Ia and peak to peak ripple voltage of the capacitor is

$$\Delta Vc = Vc - Vc\,(t = 0) = \frac{1}{c}\int_0^{t1} Ic\,dt = \frac{1}{c}\int_0^{t1} Ia\,dt = \frac{Iat_1}{c} \tag{3.32}$$

The block diagram of the DC/ DC converter is shown below in figure 3.12:

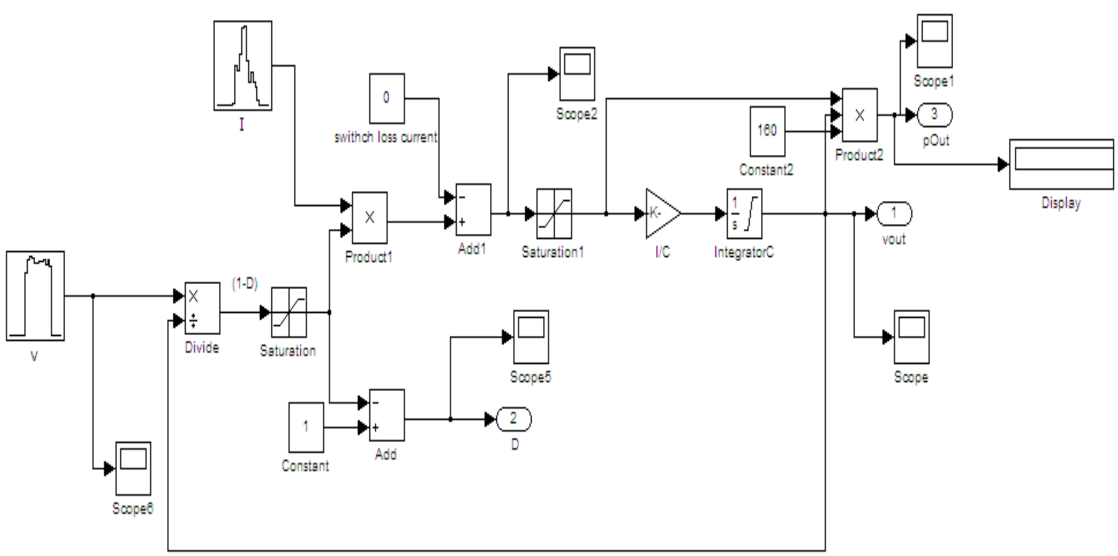

Figure 3.12: DC/DC converter of the PV system model

3.5 Complete Modeling of hybrid system

The total system of hybrid system is implemented as shown in Figure 3.13, which consists of wind turbine and photovoltaic cell system and a backup diesel generator.

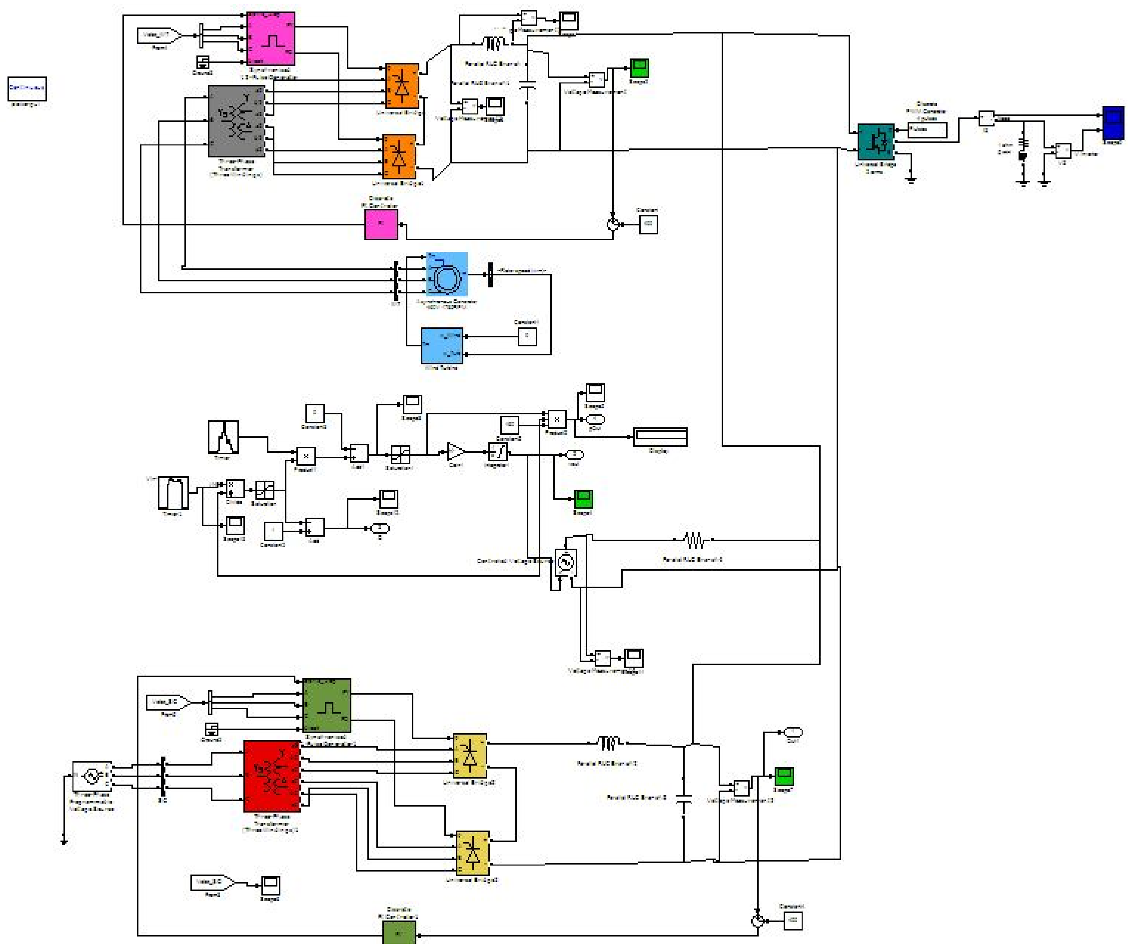

Figure 3.13: The hybrid system WT - PV and diesel system model